Wind Turbine Model-test Method for Achieving Similarity of Both Model- and Full-Scale Thrusts and Torques

Hongbin Hao[a], Kangping Liao[a,*], Qingwei Ma[b], Xing Zheng[a], Hanbing Sun[a] and Abbas Khayyer[c]

[a] College of Shipbuilding Engineering, Harbin Engineering University, Harbin, Heilongjiang, China
[b] School of Mathematics, Computer Science and Engineering, City University of London, London, UK
[c] Department of Civil and Earth Resources Engineering, Kyoto University, Kyoto 615-8540, Japan

[*]**Corresponding author:** liaokangping@hrbeu.edu.cn

Abstract

For model tests of a floating offshore wind turbine (FOWT) system, a great challenge is how to model the interaction between the wind turbine and floating platform with correctly-scaled aerodynamic and hydrodynamic loads because of a well-known contradiction between Reynolds and Froude scaling. Several approaches have been proposed in the literature to tackle the challenge but none of them can correctly and simultaneously model the scaled thrust and torque, and so the interaction between turbine and platform. This paper will present a new model-test method for achieving similarity of both thrust and torque. This is achieved by redesigning the model blades with keeping the blade twist angle same as that of the full-scale turbine and by adjusting the pitch angle of blades and rotational speed of wind turbine in model tests. Numerical simulations and wind tunnel model tests are carried out to validate the present method. Both numerical results and experimental data show that the present method can realize the similarity of thrust and torque simultaneously, and thus, making it possible to study full interaction between turbine and floating platform by physical testing in wind-wave basins.

Keywords: Wind turbine model test; Scaled thrust and torque; Reynolds and Froude similarity; FOWT

1. Introduction

The concept of FOWT (Heronemus, 1972) is a highly complex system due to the two-way coupling between hydrodynamic and aerodynamic loads on the platform and the turbine respectively, as illustrated in Fig. 1. In model tests, aerodynamic loads should be scaled based on Reynolds similarity, while hydrodynamic loads should be scaled by Froude similarity. For a FOWT model test, the contradiction between the two scaling laws makes it impossible to achieve the correctly-scaled aerodynamic and hydrodynamic loads simultaneously.

The Froude similarity is commonly used in the model tests of traditional offshore structures (Chakrabarti, 1998; Faltinsen, 1993; Sarpkaya et al., 1981), which results in a much smaller

Reynolds number in model scale than that in full scale. Therefore, the aerodynamic loads cannot be correctly scaled if the traditional Froude scaling method is applied to FOWT model test directly (Martin et al., 2014; Wen et al., 2022; Madsen et al., 2020). Therefore, a key challenge in the wind-wave basin model test of FOWT system is how to achieve the scaled aerodynamic loads correctly with a smaller Reynolds number and thus to model the interaction between turbine and floating platform in a correct way.

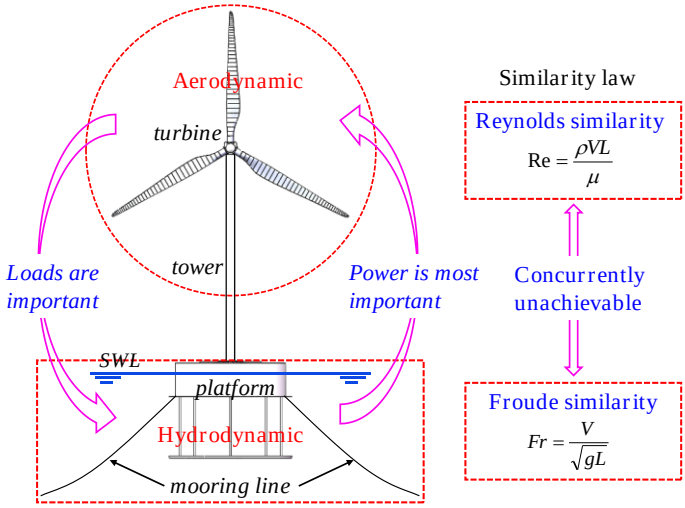

Fig. 1. Interaction between hydrodynamic and aerodynamic loads on a FOWT

There have been many studies to address the challenge and several approaches have been reviewed by Stewart et al. (2016), Chen et al. (2020) and Day et al. (2015). Some of them are summarized in Table 1.

In the early studies, the thrust force of wind turbine is simply simulated by a steady force on the top of tower. Utsunomiya et al. (2009), by using this method, tested the motion of a spar-buoy FOWT in regular and irregular waves at NMRI (National Maritime Research Institute). The method was also used by Zhao (2012) to study a semi-submersible FOWT. The steady force method can only simulate the steady thrust and so the steady displacement of platform and mooring offsets (Day et al., 2015). Clearly, this method discards the important dynamic feature of aerodynamics, and thus it only partially considers the action of the turbine on the platform.

Roddier et al. (2010) proposed a model test method using a drag disk. In their tests on WindFloat, the desired thrust was achieved by using a large disk on the top of tower. The method was also employed by Wan et al. (2015; 2016; 2016; 2017) and Gao et al. (2016). This method may be able to partially model the unsteady thrust but entirely ignores the torque.

Table 1

Approaches to simulate scaled aerodynamic loads in model tests

Approaches	Author	Similarity		Interaction between turbine and platform
		Thrust	Torque	
Steady force	Utsunomiya et al. (2009) Zhao (2012)	Partial	No	Partial effects of turbine on platform
Drag disk	Roddier et al. (2010) Wan et al. (2015; 2016; 2016; 2017) Gao et al. (2016)	Partial	No	Partial effects of turbine on platform
Geometricall y Froude scaled model	Shin (2011) Martin (2011) Koo et al. (2014) Duan (2017)	Yes	No	Turbine on platform
Redesigned blades	Martin et al. (2014) Fowler et al. (2013) Duan (2017) Du et al. (2016) Schunemann et al. (2018) Wen et al. (2020)	Yes	No	Turbine on platform
	Bayati et al. (2016; 2017; 2017)		Partially before rated wind speed	Partially both way before rated wind speed
Real-time hybrid model	Chabaud et al. (2013) Azcona et al. (2014) Sandner et al. (2015) Sauder et al. (2016) Hall et al. (2018)	Yes	No	Turbine on platform

To address the issues with the above two methods, a scaled turbine model with geometrically similar blades was used by Shin (2011), Martin (2011), Koo et al. (2014) and Duan (2017). In order to achieve the desired thrust, wind speeds were increased during the model tests (Martin, 2011; Duan, 2017). It was found that the geometrically Froude scaled model can achieve the desired thrust, but the torque was much smaller than desired. In addition, the increased wind speeds can result in extra aerodynamic loads on the tower and floating platform.

In order to achieve the desired thrust without increasing wind speeds considerably, low Reynold's blades (or geometrically distorted blades) were adopted to replace the geometrically similar blades in the model test. Martin et al. (2014) redesigned the turbine blades with the low Reynolds airfoil called Drela AG04. Their results showed that the model scale thrust was close to the full scale thrust, but the power and the torque coefficients in model scale were much smaller than those at full scale. Fowler et al. (2013) designed a turbine model with the low Reynolds airfoil named Drela AG24, which was also used by Duan (2017). With the Drela series of airfoils, the chord of the redesigned blades was enlarged excessively, which resulted in heavier blades. Low Reynolds airfoils such as NACA 4412 (Du et al., 2016), SD2030 (Schunemann et al., 2018; Wen et al., 2020) and SD7032 (Bayati et al., 2016; 2017; 2017) were considered instead. Bayati et al. (2016; 2017; 2017) designed a model using SD7032 for DTU

10MW wind turbine (Bak et al., 2013). In their redesign, they ensured that the thrust was correctly scaled, but not the torque. Nevertheless, their test results showed that the thrust was satisfactory in all test conditions, and that the torque was also approximately modelled for wind speeds less than the rated speed. As their model was not designed to achieve torque similarity, not surprisingly, the torques corresponding to the wind speeds larger than rated speed were considerably smaller than the desired values.

Another approach, called Real-time hybrid model (RTHM), has also been developed. In this approach, the wind turbine is replaced by a virtual subsystem and the desired aerodynamic thrust is realized by a feedback controlled ducted fan or actuator (Chabaud et al., 2013; Azcona et al., 2014; Sandner et al., 2015) on the top of tower. Later, Sauder et al. (2016) replaced the ducted fan with a redundant cable-based actuation system to obtain the transient simulated force with considering the effects of wind, wave and blade pitch control. This approach offers higher bandwidth and more complex loading capabilities, however, faces a great challenge in terms of complexity of equipment and controls. Then, Hall et al. (2018) used the actuation system (winch and cables, pulling fore and aft on the nacelle) and combined it with a numerical wind turbine tool to simulate the thrust.

In the FOWT system, the aerodynamics of turbine significantly affects the motions of floating platforms. On the other hand, the motions of floating platforms can also affect the aerodynamics (including thrust and torque) of turbines. The interaction between them plays an important role in determining the dynamic behaviors of the whole FOWT systems. In the state-of-art studies, most approaches of model tests can only model turbine's effects (i.e., thrust) to some extent. Only the approach proposed by Bayati et al. (2016; 2017; 2017) can approximately model the interaction at wind speeds smaller than the rated speed. To the best knowledge of the authors, no model-test method has been suggested to correctly and simultaneously model the scaled thrust and torque, and so the interaction between turbine and platform based on the Froude similarity law.

This paper will propose a scaled model test method, which can achieve the similarity of both thrust and torque in the whole range of wind speeds. This will establish a foundation for realizing the correct modelling of the interaction between turbine and platform during the tests of FOWT models in wind-wave basins. For the ease of discussions, a scale model of DTU 10MW (Bak et al., 2013) wind turbine with scale factor 1:100 is designed by the present method. The proposed method is verified by the numerical and experimental results.

2. Description of wind turbine model-test method

In the model test of FOWT systems in wind-wave basins, the interaction between turbine and floating platform mainly happens in two ways. One is the influence of turbine's aerodynamic loads (mainly the thrust) on the motion of platform, the other is the influence of platform's motion on the aerodynamic loads (mainly the thrust and torque) of turbine. To make it possible to study the full interaction by physical testing in wind-wave basins, the thrust and torque of turbine should be well scaled firstly.

To achieve the similarity of scaled thrust and torque simultaneously in model tests, the thrust and torque coefficients of the model and its full-scale counterpart must be the same

$$C_T = \frac{T_F}{0.5\rho V_{w-F}^2 S_F} = \frac{T_M}{0.5\rho V_{w-M}^2 S_M} \tag{1}$$

$$C_Q = \frac{Q_F}{0.5\rho V_{w-F}^2 S_F R_F} = \frac{Q_M}{0.5\rho V_{w-M}^2 S_M R_M} \tag{2}$$

in which, ρ is the density of air, V_w is the wind speed, S and R are the area and radius of rotor's rotational annular plane, respectively. The subscripts F and M denote the full scale and model scale, respectively.

The aerodynamic performance of wind turbines can be affected by many factors. These include the geometrical parameters of blade, such as of the blade chord (c), twist angle (β) and relative thickness (t/c) distribution along the blade span. The other factors include the operational parameters, such as the blade pitch angle (θ) and the rotational speed (ω).

Generally, a model test of FOWT system is designed based on the Froude similarity, which does not satisfy the Reynolds similarity. Therefore, in the FOWT model tests, the Froude scaled wind turbine may not provide correct thrust and torque to the floating platform. One approach to overcome this inconsistency was proposed by Bayati et al. (2016) as indicated before. In their approach, the low Reynolds blade was used which is geometrically unsimilar to the full-scale blades. Main assumptions in their method were: (1) the inflow angle ϕ of the model is the same as that of the full-scale counterpart; (2) the blade pitch angle θ is also the same in full scale and model scale; (3) the drag force on the blade in model scale is ignored when designing the model. The results by Bayati et al. (2016) showed that the model scale wind turbine with the low Reynolds blade can achieve the correctly-scaled thrust. However, it is difficult to achieve the scaled torque in the high wind speed region larger than the rated wind speed. In this study, we will propose an approach which can address this issue. Compared to the method of Bayati et al. (2016), the proposed approach assumes that the twist angle in the model scale, instead of pitch angle, is the same as that in the full scale. This assumption will make it easy to

145 determine the blade geometrical characteristics, and to obtain the lift and drag coefficients more
146 accurately. In addition, this new approach will consider both of lift and drag forces on the blade,
147 which help achieving the correctly-scaled thrust and toque simultaneously.

148 *2.1 Method for designing the geometry of low Reynolds blade*

149 As mentioned before, a low Reynolds blade for the model scale needs to be designed in
150 FOWT model tests. The key issue of low Reynolds blade design is to determine the blade's
151 geometrical parameters, such as chord (c_M), twist angle (β_M) and relative thickness (t/c)
152 distribution along the blade span. As indicated before, the model twist angle is taken to be the
153 same as the full scale. The relative thickness (t/c) distribution is determined in the same way as
154 Bayati et al. (2016). The following discussion is presented on how to determine the chord length
155 of the model blades.

156 In the present method, similar to Bayati et al. (2016), the inflow angle is assumed to be the
157 same in model and full scales, i.e.

158 $$\phi_M = \phi_F \tag{3}$$

159 Differently from the reference (Bayati et al., 2016), we assume that the twist angle (β),
160 instead of pitch angle (θ), is the same in the model and full scales,

161 $$\beta_M = \beta_F \tag{4}$$

162 To determine the chord length (c_M) along the blade span, we will employ a two-step approach.
163 In the first step, the preliminary chord (c_{M0}) is obtained directly by matching the scaled lift force
164 along the blade span.

165 Considering the airfoil section in Fig. 2, the angle of attack α is given by

166 $$\alpha = \phi - (\beta + \theta) \tag{5}$$

167 Based on the airfoil theory, the lift and drag acting on the airfoil section are

168 $$L = 0.5\rho c dr V_{rel}^2 \cdot Cl(\alpha) \tag{6}$$

169 $$D = 0.5\rho c dr V_{rel}^2 \cdot Cd(\alpha) \tag{7}$$

170 where, ρ is the density of air, dr is the span of the blade element, $Cl(\alpha)$ and $Cd(\alpha)$ are the lift
171 and drag coefficients, respectively. In the linear region (i.e. small angle of attack) of an airfoil
172 lift curve, the lift coefficient can be approximated as

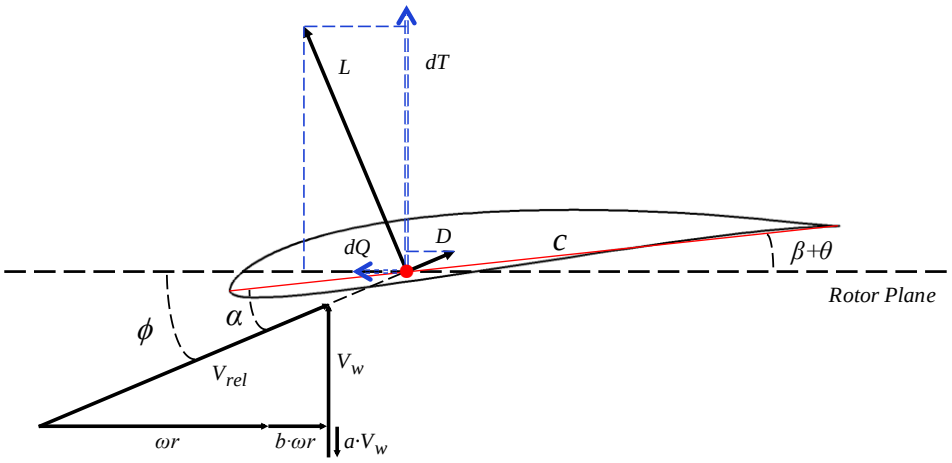

Fig. 2. Aerodynamic forces on airfoil section

$$Cl(\alpha) = kl \cdot \alpha + Cl^0 = kl \cdot (\phi - \beta - \theta) + Cl^0 \tag{8}$$

in which, kl is the slope of airfoil lift curve in the linear region and Cl^0 is the lift coefficient when the angle of attack is zero.

According to the similarity theory, the relationship of lift forces between full scale (L_F) and model scale (L_M) is

$$L_F = \lambda_L^2 \lambda_V^2 \cdot L_M \tag{9}$$

where λ_L is the dimensional scale factor, equal to the ratio of full scale length to model scale length; λ_V is the velocity scale factor, equal to the ratio of velocity of full scale to that of model scale. If the Froude law is followed, $\lambda_V = \sqrt{\lambda_L}$. However, in practice, λ_V is determined, not by following the Froude law, but by considering the wind-speed generation capability in laboratory and by making the test cases with Reynolds number closer to that of full scale, as suggested by Bayati et al. (2016).

Substituting Eqs. (3-8) into Eq. (9), one gets

$$c_F[kl_F(\phi - \beta - \theta_F) + Cl_F^0] = \lambda_L \cdot c_{M0}[kl_M(\phi - \beta - \theta_M) + Cl_M^0] \tag{10}$$

Taking the derivative of Eq. (10) with respect to β, we obtain

$$c_F \cdot kl_F = \lambda_L \cdot c_{M0} \cdot kl_M \tag{11}$$

Thus, the preliminary model scale airfoil chord of the blade element is given by

$$c_{M0} = \frac{c_F}{\lambda_L} \cdot \frac{kl_F}{kl_M} \tag{12}$$

which is the same as used by Bayati et al. (2016), though the twist angle is assumed to be same for full scale and model scale in this study, while Bayati et al. (2016) assumed that the pitch angle is the same as indicated before.

As sketched in Fig. 2, the thrust (dT) and torque (dQ) of a blade element can be estimated by

$$dT = L\cos\phi + D\sin\phi \tag{13}$$

$$dQ = (L\sin\phi - D\cos\phi)\cdot r \tag{14}$$

According to Eqs. (13-14), it is clear that the correctly-scaled thrust and torque can be achieved simultaneously when the airfoil lift-drag ratio and inflow angle are the same in full scale and model scale. However, the airfoil lift-drag ratio is generally different in full scale and model scale, since the low Reynolds blade is used in model tests. To make better matching of thrust and torque, a correction factor γ is introduced to Eq. (12) in the second step, as follows:

$$c_M = \gamma\cdot c_{M0} = \gamma\cdot\frac{c_F}{\lambda_L}\cdot\frac{kl_F}{kl_M}. \tag{15}$$

In order to evaluate γ, the torques in full scale and model scale are considered

$$dQ_F = (L_F\sin\phi - D_F\cos\phi)\cdot r_F = 0.5\rho c_F V_{rel-F}^2[Cl_F(\alpha_F)\sin\phi - Cd_F(\alpha_F)\cos\phi]r_F dr_F \tag{16}$$

$$dQ_M = (L_M\sin\phi - D_M\cos\phi)\cdot r_M = 0.5\rho\gamma c_{M0} V_{rel-M}^2[Cl_M(\alpha_M)\sin\phi - Cd_M(\alpha_M)\cos\phi]r_M dr_M. \tag{17}$$

To fulfill the similarity in torque, they need to satisfy

$$dQ_F = \lambda_L^{\,3}\lambda_V^{\,2}\cdot dQ_M \tag{18}$$

Substituting Eqs. (16-17) into Eq. (18), the correction factor can be determined as

$$\gamma = \frac{\tan\phi - 1/K_F(\alpha_F)}{\tan\phi - 1/K_M(\alpha_M)} = \frac{\tan\phi - Cd_F(\alpha_F)/Cl_F(\alpha_F)}{\tan\phi - Cd_M(\alpha_M)/Cl_M(\alpha_M)}. \tag{19}$$

For estimating the value of γ in a simple way, α_F is taken to be the attack angle at the blade tip corresponding to the rated wind speed, and ϕ is taken to be the inflow angle at the tip of blade, ignoring the induced velocities, i.e.

$$\phi \approx arc\cot(TSR_D), \tag{20}$$

where the TSR_D is the tip-speed ratio at design condition of the full-scale turbine.

According to Eqs. (10-11)

$$\alpha_M = \alpha_F + \frac{Cl_F^{\,0}}{kl_F} - \frac{Cl_M^0}{kl_M}. \tag{21}$$

Substituting Eqs. (20-21) into Eq. (19), one gets

$$\gamma = \frac{\dfrac{1}{TSR_D} - \dfrac{Cd_F(\alpha_F)}{Cl_F(\alpha_F)}}{\dfrac{1}{TSR_D} - \dfrac{Cd_M(\alpha_F + Cl_F^{\,0}/kl_F - Cl_M^0/kl_M)}{Cl_M(\alpha_F + Cl_F^{\,0}/kl_F - Cl_M^0/kl_M)}}. \tag{22}$$

One benefit of the present method is that the re-designed low Reynolds blade does not depend

on the pitch angle which varies with wind speeds and can be applied in various model test conditions.

2.2 Method for adjusting the pitch angle and rotational speed

In order to produce correct thrust and torque simultaneously in laboratory tests using the turbine model discussed above, the blade pitch angle and rotational speed must be properly adjusted. This section will describe the method for determining the pitch angle and rotational speed.

As well known, the relative axial wind speed and rotational speed can be given by

$$V_{in} = (1-a)V_{w-M} \qquad V_r = (1+b)r_M \cdot \omega_M \tag{23}$$

where *a* and *b* are the induced factor of axial velocity and tangential velocity, respectively.

The resulting inflow velocity and inflow angle will be expressed by

$$V_{rel-M} = \sqrt{[(1-a)^2 V_{w-M}^2 + (1+b)^2 (r_M \cdot \omega_M)^2} \tag{24}$$

$$\phi_M = ar\cot\frac{(1+b)r_M \cdot \omega_M}{(1-a)V_{w-M}} \tag{25}$$

Substituting Eqs. (24-25) in Eqs.(13-14), one gets the thrust and torque components on a blade element as

$$dT_M = 0.5\rho c_M V_{rel-M} \cdot [(1+b)\omega_M r_M \cdot Cl_M(\alpha_M) + (1-a)V_{w-M} \cdot Cd_M(\alpha_M)] \cdot dr_M \tag{26}$$

$$dQ_M = 0.5\rho c_M V_{rel-M} \cdot [(1-a)V_{w-M} \cdot Cl_M(\alpha_M) - (1+b)\omega_M r_M Cd_M(\alpha_M)] \cdot r_M \cdot dr_M \tag{27}$$

It is noted that the relationship between lift coefficient and attack angle used in Eqs. (26-27) is the real function, instead of the approximated linear relationship. And the more accurate the relationship between the attack angle and the coefficients is, the more accurate the thrust and torque will be.

In order to evaluate the induced velocity factors, the momentum theory will be applied. For a model with *B* blades, the thrust on a blade element based on momentum equation is

$$dT = \frac{1}{2}\rho S_M V_{w-M}^2 4a(1-a) = \frac{1}{2}\rho(2\pi r_M dr_M)V_{w-M}^2 4a(1-a) = B \cdot dT_M \tag{28}$$

where $S_M = 2\pi r_M \cdot dr_M$ is the area of rotational annular plane.

Similarly, the torque of a blade element is

$$dQ = (2\pi r_M dr_M \rho V_{in})V'_r r_M = 4\pi\rho\omega_M b(1-a)V_{w-M} r_M^3 dr_M = B \cdot dQ_M \tag{29}$$

in which, $V'_r = 2b\omega_M r_M$ is the induced tangential velocity.

Combining Eqs. (26-29), one obtains

$$\frac{a}{1-a}=\frac{\sigma[Cl_M(\alpha_M)\cos\phi_M+Cd_M(\alpha_M)\sin\phi_M]}{4\sin^2\phi_M} \tag{30}$$

$$\frac{b}{1+b}=\frac{\sigma[Cl_M(\alpha_M)\sin\phi_M-Cd_M(\alpha_M)\cos\phi_M]}{4\sin\phi_M\cos\phi_M} \tag{31}$$

where $\sigma=\frac{Bc_M}{2\pi r_M}$ is the turbine solidity.

When the Prandtl tip loss correction factor is considered, Eqs. (30-31) can be rewritten as

$$\frac{a}{1-a}=\frac{\sigma[Cl_M(\alpha_M)\cos\phi_M+Cd_M(\alpha_M)\sin\phi_M]}{4f\sin^2\phi_M} \tag{30-1}$$

$$\frac{b}{1+b}=\frac{\sigma[Cl_M(\alpha_M)\sin\phi_M-Cd_M(\alpha_M)\cos\phi_M]}{4f\sin\phi_M\cos\phi_M} \tag{31-1}$$

in which, $f=\frac{2}{\pi}ar\cos[\exp(-\frac{B}{2}\frac{R_M-r_M}{r_M\sin\phi_M})]$.

The total thrust and torque of the scaled turbine model can be calculated from Eqs. (26-27) by

$$T_M=B\cdot\int_0^{R_M}dT_M=0.5B\rho\cdot\int_0^{R_M}c_M V_{rel-M}\cdot[(1+b)\omega_M r_M Cl_M(\alpha_M)+(1-a)V_{w-M}Cd_M(\alpha_M)]dr_M \tag{32}$$

$$Q_M=B\cdot\int_0^{R_M}dQ_M=0.5B\rho\cdot\int_0^{R_M}c_M V_{rel-M}\cdot[(1-a)V_{w-M}\cdot Cl_M(\alpha_M)-(1+b)\omega_M r_M Cd_M(\alpha_M)]\cdot r_M\cdot dr_M \tag{33}$$

It indicates that the thrust and torque are functions of θ_M and ω_M.

According to Eqs. (1-2), one has

$$T_M=T_F/\lambda_L^2\lambda_V^2, \tag{34}$$

$$Q_M=Q_F/\lambda_L^3\lambda_V^2. \tag{35}$$

Solving them together, the pitch angle θ_M and rotational speed ω_M can be determined for each wind speed. In the equations, T_F and Q_F are assumed to be given. If that would not be the case, one can estimate them using numerical tools.

The model test method for achieving similarity of both thrust and torque of model- and full-scale wind turbines is summarized in Fig. 3. It will be validated with numerical and experimental results in the following section.

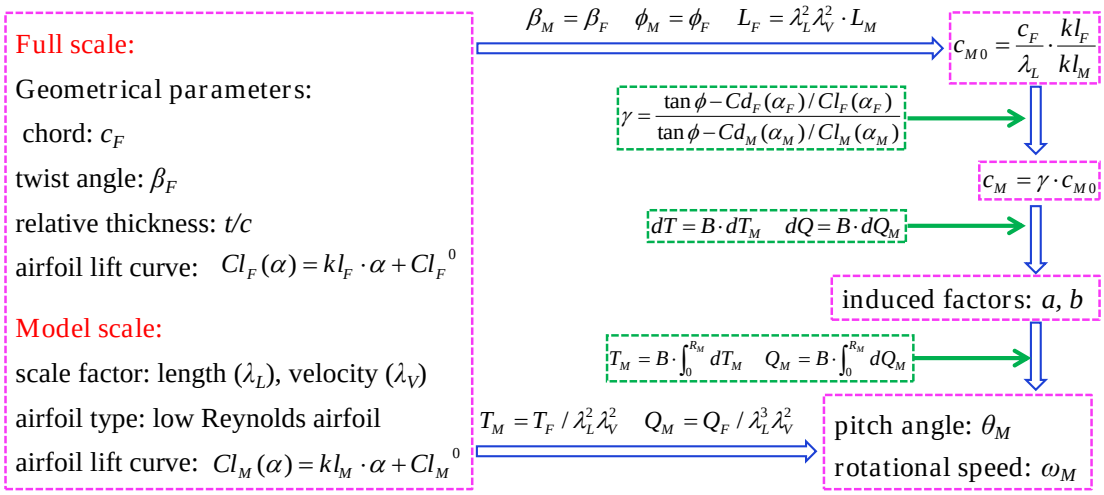

Fig. 3. Wind turbine model-test method

The main features of the present method and its difference from that presented by Bayati et al. (2016) are summarized in Table 2. There is one point to be further discussed here, which is about the rotational speed. In the present method, the rotational speed is determined using Eqs. (34-35) to ensure the similarity of both thrust and torque while it was determined by $\omega_F \lambda_V / \lambda_L$ in Bayati et al. (2016). The Froude scaling of rotational speed should be $\omega_F / \sqrt{\lambda_L}$. The results below will show that the rotational speed from Eqs. (34-35) is in the range of $\omega_F / \sqrt{\lambda_L} < \omega_M < \omega_F \lambda_V / \lambda_L$ at least for the cases considered. The choice of $\omega_F \lambda_V / \lambda_L$ by Bayati et al. (2016) ensures that the Tip Speed Ratio (TSR) is the same for both model and full scales, which is not the case in the present method. Certainly, a mismatching in the TSR together with other parameters such as the Froude number for air, blade geometry and so on will lead to inconsistence of the detailed aerodynamics between model- and full-scale turbines. Nevertheless, the present method realizes the similarity of both thrust and torque, which are important for studying the interaction between turbine and floating platform by physical tests in wind-wave basin.

Table 2

Comparison of main features of different scaling methods

Main Parameters of scaled model	Method in Bayati et al. (2016)	Present method
Thrust	correctly scaled	correctly scaled
Torque	incorrectly scaled at high speed	correctly scaled
Tip Speed Ratio	correctly scaled	incorrectly scaled
Twist angle	incorrectly scaled	correctly scaled
Pitch angle	correctly scaled	incorrectly scaled
Rotational speed	incorrectly scaled	incorrectly scaled
Blade section	incorrectly scaled	incorrectly scaled

Turbine diameter	correctly scaled	correctly scaled

3. Numerical validation of wind turbine model-test method

The present method is firstly validated by using the commercial CFD software Star-CCM+ (Siemens, 2017). For ease of discussions, a scaled model of DTU 10MW (Bak et al., 2013) wind turbine with scale factor 1:100 is re-designed by the present method. Then, the thrust and torque with different velocity scale factors are calculated. In preparation for the model test of FOWT system in wind-wave basins, the wind speeds are selected by considering the wind-speed generation capability in wave basins.

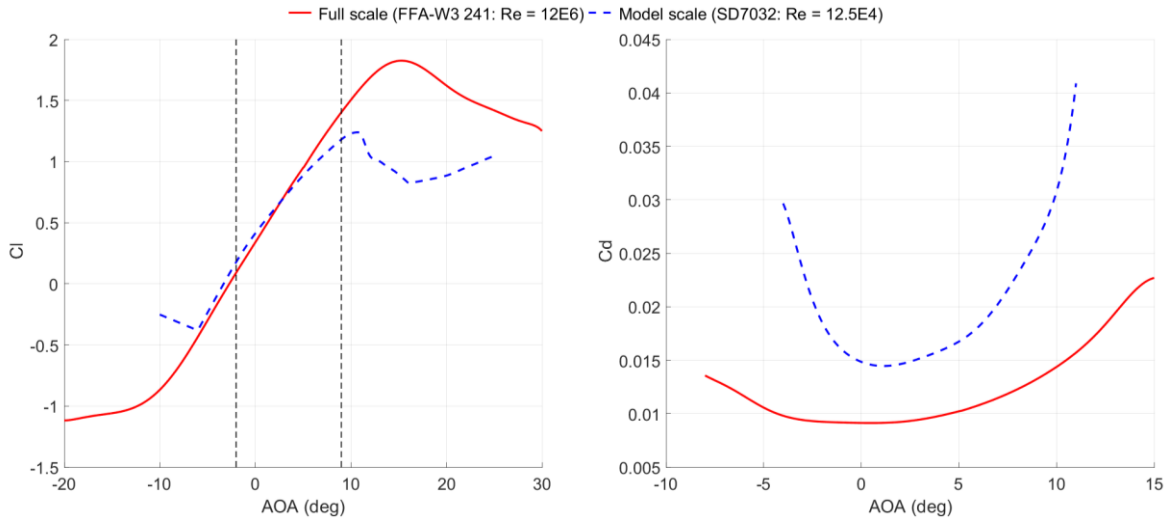

Fig. 4. Lift curves of airfoil used in full scale and model scale blades

3.1 Design of model scale wind turbine

In this study, the Selig-Donovan low Reynolds airfoil SD7032 following Bayati et al. (2016) is employed and the corresponding Reynolds number is about 12.5×10^4. Comparisons of the airfoil lift and drag coefficients between model- and full-scale airfoils are shown in Fig. 4. It can be seen that the airfoil in full scale and model scale blades have obviously different stall angles, which are about 15° and 11°. In standard working condition, most length of full scale blades works far from stall and the attack angle is about in the range of [-2, 9]. For this range, the lift coefficients of airfoil in full scale and model scale blades are approximately linear, and the slope of the former is larger than the latter. According to Eq. (12), the chord of preliminary model scale airfoil chord of the blade element will be larger than the geometric scaled one.

According to Eq. (8), the lift curves can be approximated as a linear relationship to angle of attack

$$Cl_F(\alpha_F) = kl_F \cdot \alpha_F + Cl_F^0 = 0.1201 \cdot \alpha_F + 0.34233 \tag{36}$$

$$Cl_M(\alpha_M) = kl_M \cdot \alpha_M + Cl_M^0 = 0.08766 \cdot \alpha_M + 0.42751 \tag{37}$$

According to Eq. (12), the preliminary model scale airfoil chord is

$$c_{M0} = \frac{c_F}{\lambda_L} \cdot \frac{kl_F}{kl_M} = 1.37 \cdot c_F / \lambda_L \tag{38}$$

With the enlarged factor (Eq.22) at the rated wind speed equal to 1.0836, one obtains

$$c_M = \gamma \cdot c_{M0} = 1.4845 \cdot c_F / \lambda_L \tag{39}$$

The relative thickness distribution is determined in the same way as Bayati et al. (2016). With using the same twist angle as that of full scale blades, the model scale blade can be obtained, as shown in Fig. 5.

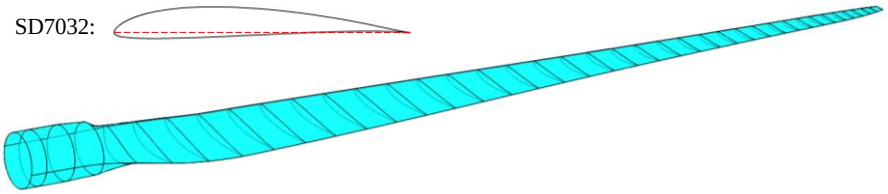

Fig. 5. Redesigned model scale blade with the present method

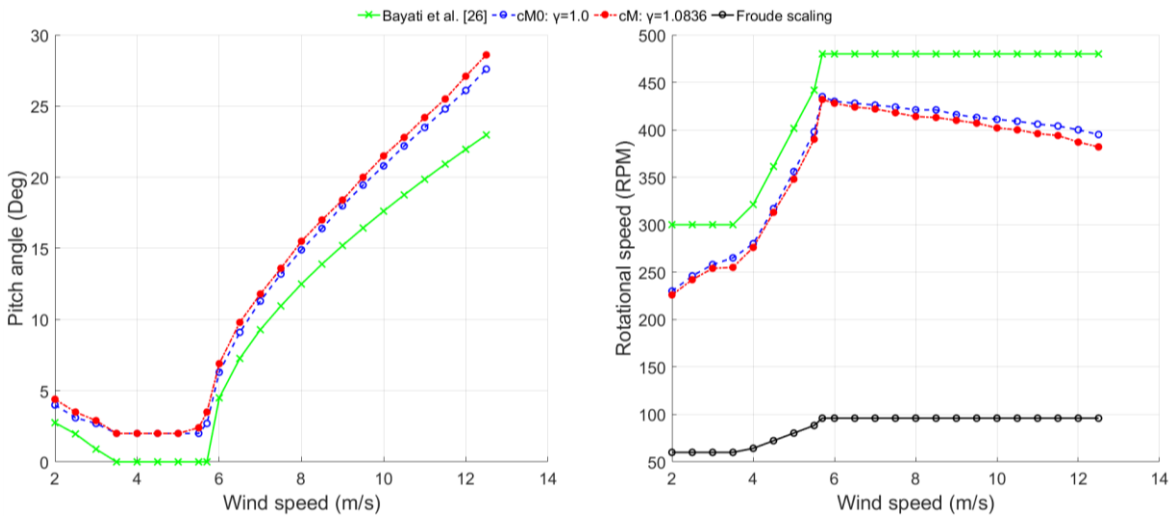

Fig. 6. Pitch angle and rotational speed for different wind speeds (λ_V = 2)

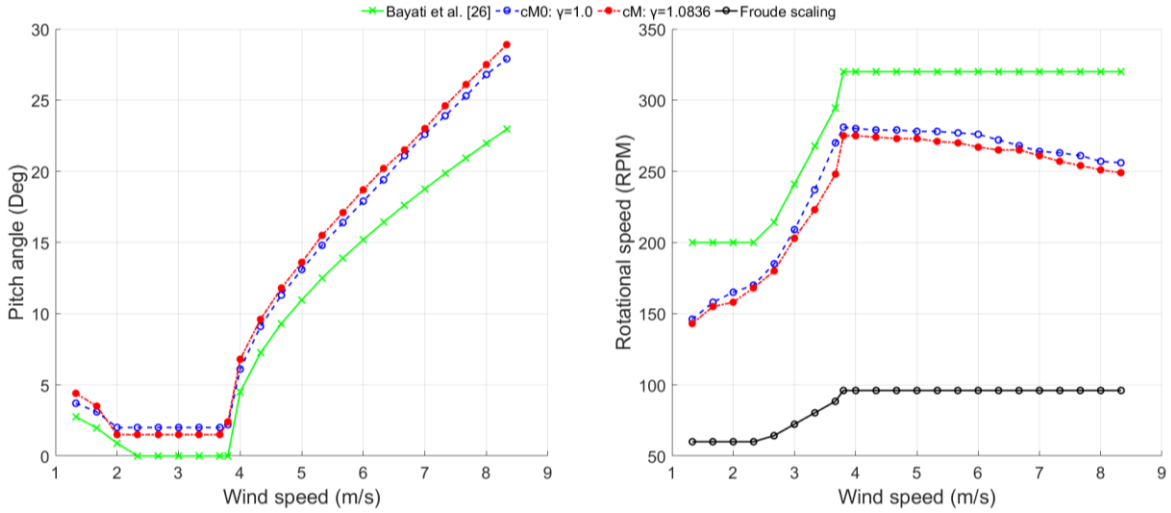

Fig. 7. Pitch angle and rotational speed for different wind speeds ($\lambda_V = 3$)

The pitch angle and rational speed can be determined from Eqs. (34-35) as mentioned before. Fig.6 and Fig.7 show the results for $\lambda_V = 2$ and $\lambda_V = 3$, respectively. In the figures, the green solid lines present the results obtained with the method proposed by Bayati et al. (2016), the black solid line is obtained with direct Froude scaling, while the red dash-dotted lines and blue dashed lines are obtained with the present method. This clearly shows the rotational speeds of the present method is in between that used by the Bayati et al. (2016) and that based on the full Froude scaling.

3.2 Computational set-up and validation

In order to ensure that the results of Star-CCM+ are credible, the aerodynamic forces of full scale DTU 10MW wind turbine are calculated and compared with the reference results firstly. The computational domain setup is shown in Fig. 8. The maximum mesh size is about 0.23*R*, and the mesh is encrypted to a maximum size of 0.057*R* near the wind turbine. The maximum and minimum size on the surface of blade is about 0.0018*R* and 0.00022*R* respectively, 2 layers of boundary layer mesh are generated with a total layer thickness of 0.0007R and a progression factor of 1.2. The total number of cells in the computational domain is about 1.73×10^6.

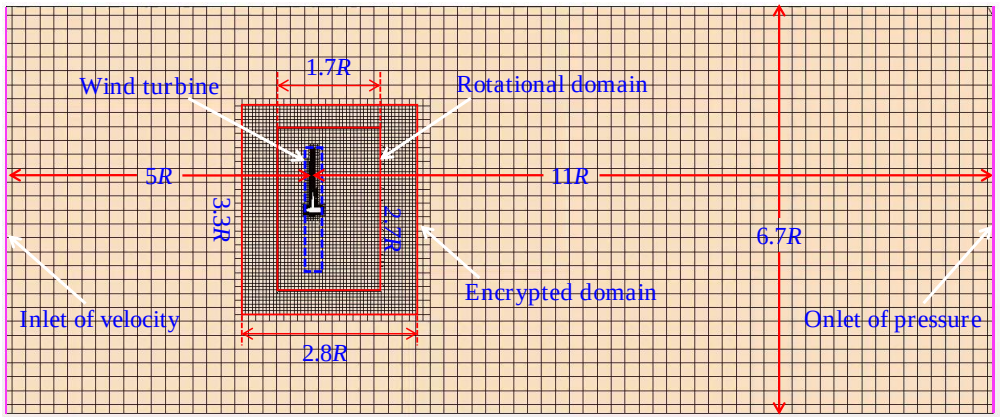

Fig. 8. Computational setup

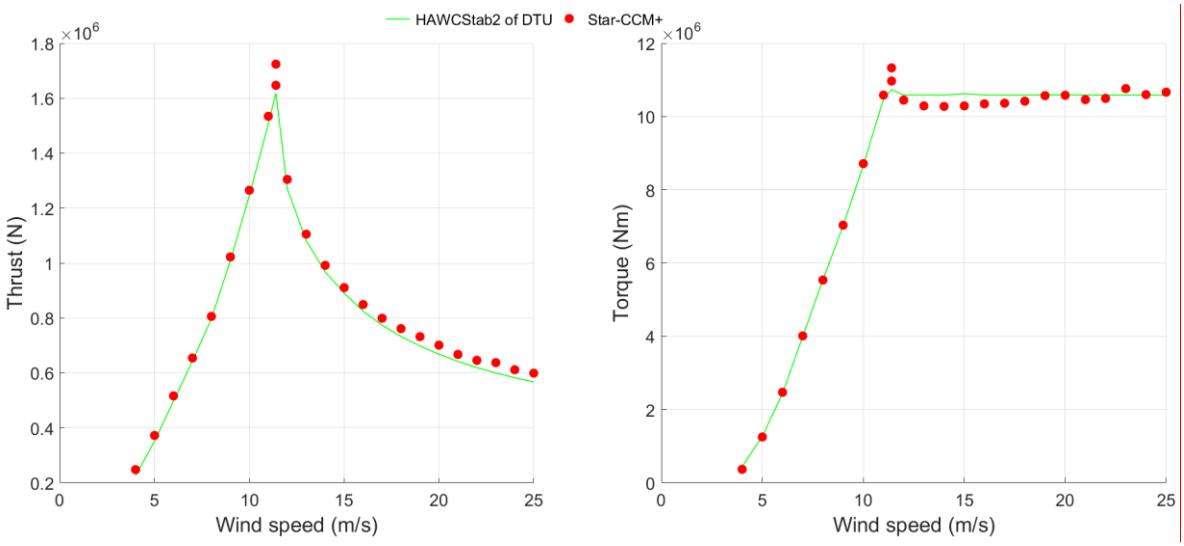

Fig. 9. Thrust and torque of full scale DTU-10MW wind turbine for different wind speeds

The thrust and torque of full scale DTU-10MW wind turbine against wind speed are shown in Fig. 9. In this figure, the green solid lines present the results obtained by HAWCStab2 (Bak et al., 2013), while the red points are the results obtained by Star-CCM+ in this study. It should be noted that there are two points when the wind speed is 11.4m/s, which is the rated wind speed of full scale DTU-10MW wind turbine. One point is the results with the rotational speed of 9.16rpm, and the other is the results with the rotational speed of 9.6rpm. In fact, the rated wind speed is the critical state of full scale DTU-10MW wind turbine. As known, the TSR (7.5) is kept when the wind speed is less than the rated one, and the maximum power coefficient is used to capture the wind energy. By this way, the rotational speed at the rated wind speed should be 9.16rpm, the thrust and torque will be the smaller and larger values respectively. However, the maximum rotational speed (9.6rpm) is kept when the wind speed is larger than the rated one, and the rated power is used to capture the wind energy. By this way, the rotational speed

at the rated wind speed should be 9.6rpm, and the thrust and torque will be the larger and smaller values respectively. From the figure, it can be seen that the results of Star-CCM+ agree well with the results of HAWCStab2 which is based on BEM, the errors for all considered wind speeds do not exceed 6.5%. Fig. 9 indicates that the results of Star-CCM+ are credible.

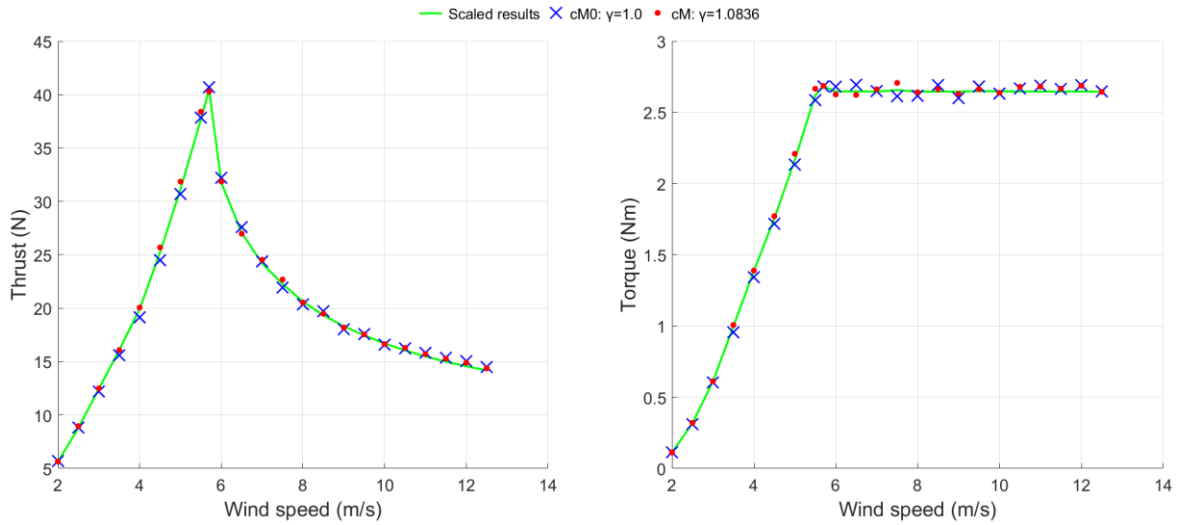

Fig. 10. Thrust and torque for different wind speeds (λ_V = 2)

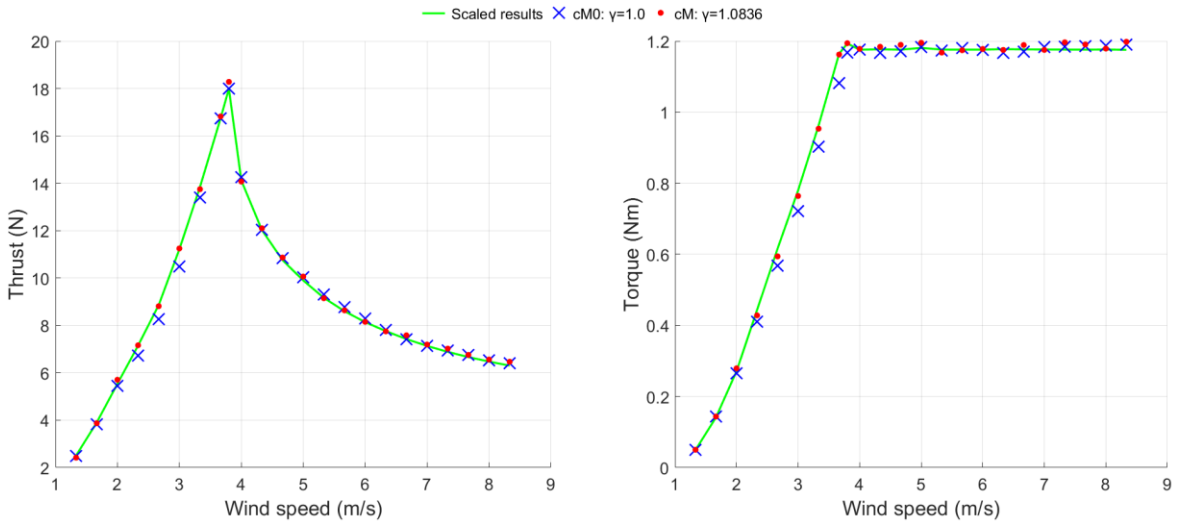

Fig. 11. Thrust and torque for different wind speeds (λ_V = 3)

3.3 Numerical results of the model scale wind turbine

Fig. 10 presents the thrust and torque of the redesigned model scale wind turbine with velocity scale factor 2. The green solid lines are the directly scaled results obtained by Eqs. (34-35), the blue crosses are obtained by the present design method with the airfoil chord c_{M0} defined in Eq.(38), and the red points are obtained by the present design method with the airfoil

chord c_M defined in Eq.(39). With the scaled pitch angle and rotational speed, shown in Fig. 6, the scaled thrust and torque can be achieved simultaneously in the whole range of wind speeds. It should be noted that, in low wind speed region (i.e. lower than rated wind speed), the result with c_M is in better agreement with the directly scaled result (i.e. the green solid line) than that with c_{M0}. As we know, in the low wind speed region, the angle of attack is commonly close to the one with the maximum lift coefficient. To achieve enough thrust and torque, the airfoil chord should be slightly larger since the lift-drag ratio of the redesigned low Reynolds blade is relatively low. This is the possible reason why the result with c_M shows to be better than that with c_{M0}.

A scaled wind turbine with velocity scale 3 is also carried out to check whether the redesigned blade obtained by the present method is suitable for cases with different velocity scale factor. It is clear that the scaled thrust and torque can also be achieved simultaneously in the case with velocity scale 3, as shown in Fig. 11. It indicates that the redesigned blades obtained by the present method can be used for cases with different velocity scale factors. The only thing we should do is to adjust the pitch angle and rotational speed for different cases, as shown in Fig. 7.

Fig. 12. Physical model of redesigned blade

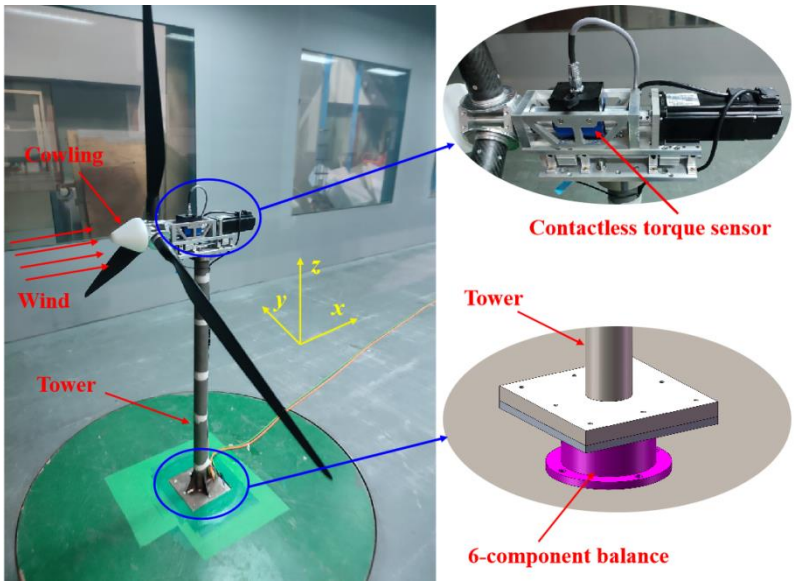

Fig. 13. Experimental setup

4. Experimental validation of wind turbine model-test method

For the model test of wind turbines in wind tunnel, the increased wind and rotational speeds are generally used to maintain the Reynolds scaling. In this paper, the wind tunnel test is to further validate the present method and preparing for the model test of FOWT system in wind-wave basins. Therefore, the wind speeds which can be realizable by the wind generating system in wave basin are employed. And the velocity scale factor in wind tunnel test is 2.

The model test is carried out in a boundary layer wind tunnel, which has the dimensions of 18m × 4m × 3m. The physical model of redesigned low Reynolds blade is shown in Fig. 12, and the experimental setup is shown in Fig. 13. In experiment, the thrust is measured by a 6-component balance under the bottom of tower and the torque is measured by a contactless torque sensor on rotation axis.

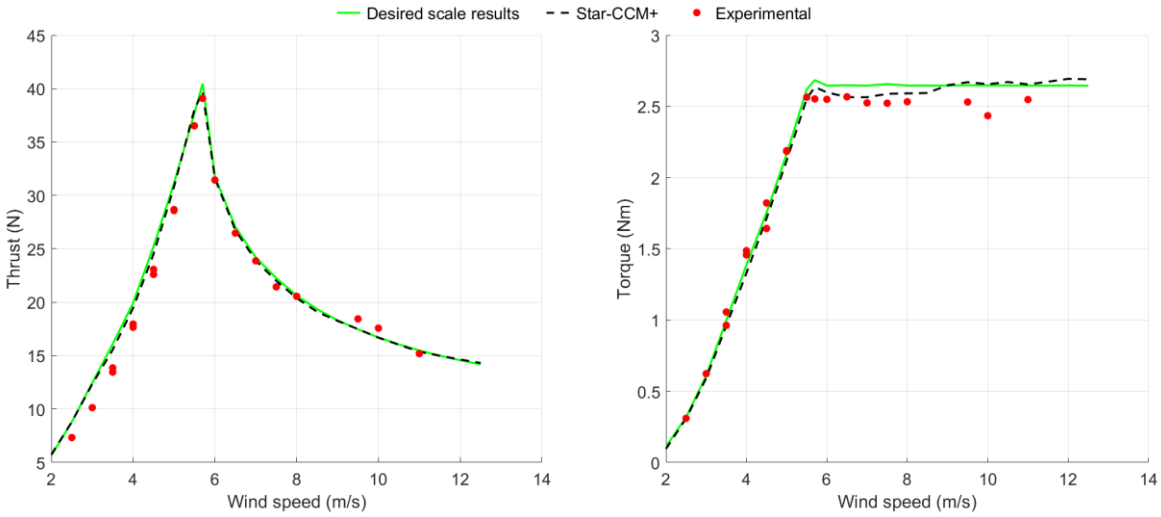

Fig. 14. Experimental results of model scale wind turbine for different wind speeds

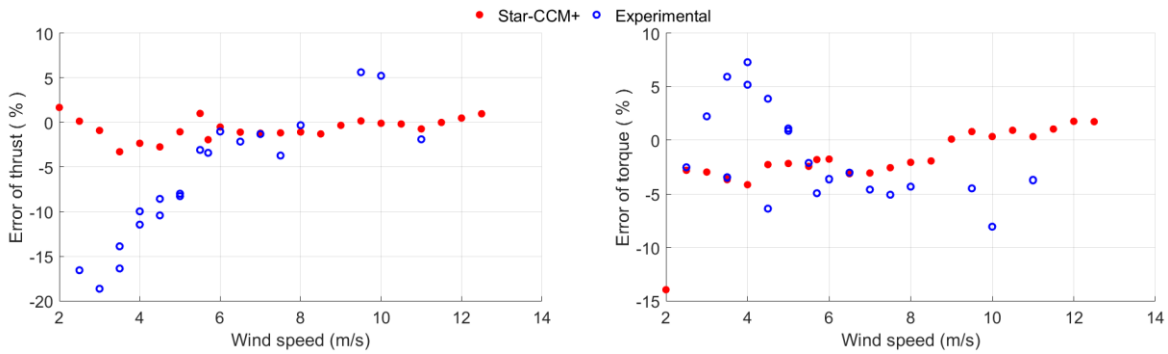

Fig. 15. Experimental-numerical errors of thrust and torque relative to scaled results

The experimental results when the velocity scale factor equals to 2 are shown in Fig. 14. In the figure, the green solid lines are the directly scaled results obtained by Eqs. (34-35). They

are also the desired scale thrust and torque of model scale wind turbine for different wind speeds. The operating conditions in experiment are also solved based on the green solid lines. The red points are the results of experiment and the black dashed lines are obtained with Star-CCM+ by using the operating condition in experiment. It can be seen that the results of Star-CCM+ agree well with the experimental results for most of the wind speeds, which further indicates that the results of Star-CCM+ are credible.

Fig. 15 shows the error relative to the desired scale thrust and torque (green lines in Fig. 14). It can be seen that the results of Star-CCM+ agree very well with the desired scale results, and most of the errors are less than 4%. The numerical results indicate that the operating conditions in experiment are credible and they can make the model scale wind turbine achieve the desired scale thrust and torque simultaneously.

When the wind speed is less than the rated wind speed (5.7m/s), the experimental results have the same trends as the desired scale results, obtained with Eq. (34-35). Although the experimental thrust force is smaller than the scaled value, most of the errors are less than 10% which are acceptable. In addition, the scaled torque is also achieved simultaneously. When the wind speed is larger than the rated wind speed, the experimental thrust force agrees well with the scaled value. And the experimental torque is smaller than the scaled value, however, most of the errors are less than 5%. In summary, although the thrust and torque do not agree excellently with the desired scale results, the corresponding errors can be considered as acceptable. To the best of our knowledge, no other model test methods can achieve similarity of both thrust and torque at high wind speed, greater than the rated wind speeds.

From Fig. 14, the only major discrepancies in between the results of experiment and Star-CCM+ correspond to the wind speed conditions of 9m/s~11m/s. This may be caused by the variation of relative inflow velocity. In Star-CCM+, the wind speed is uniform and the wind turbine is rigid. While in physical experiment, the wind speed is not necessarily uniform and completely stable. Besides, the 6-component balance under the tower is a flexible structure, which makes the tower vibrate obviously with the increasing of wind speed. As a result, the attack angles of blade elements will oscillate around its equilibrium position. Under the wind speed conditions of 9m/s~11m/s, the attack angles of more than 50% of blade span are negative. According to the lift and drag curves of airfoil used in model scale blades (Fig. 4), the vibration of attack angle will lead to the decreasing and increasing of lift and drag component respectively. According to Eq. (13) and Eq. (14), the torque of wind turbine will be less obviously than the results of Star-CCM+.

5. Conclusions and discussions

In this study, a wind turbine model-test method is proposed for achieving similarity of both model- and full-scale thrust and torque. This is achieved by redesigning the model blades and by adjusting the pitch angle of the blades and rotational speed of the turbine. In the present method, the model blade is redesigned by keeping its twist angle, instead of pitch angle, same as that of the full-scale blades, which makes it possible for the model to suite a wide range of wind speeds. In addition, this new approach considers both lift and drag forces when determining the chord length of the airfoil of the model blade, which helps achieving the correctly-scaled thrust and toque. During model tests, the pitch angle of the blades and the rotational speeds of turbine are adjusted by ensuring that overall torque and thrust are similar for both model- and full-scale turbines in the full range of wind speeds up to the cut-off speed.

Numerical simulations and wind tunnel model tests are carried out to validate the new method. In the numerical validation, two scaled wind turbines with different velocity scale factors, i.e. $\lambda_V = 2$ and $\lambda_V = 3$, are simulated by the CFD software Star-CCM+. Numerical results show that the correctly scaled thrust and torque can be achieved simultaneously for all the wind speeds under which the turbine would be operated for both the velocity scale factors. In the experimental validation, a scaled wind turbine with velocity scale factor $\lambda_V = 2$ is tested in a boundary layer wind tunnel. The results demonstrate that the proposed method can realize the similarity of thrust and torque simultaneously for all the wind range of speeds.

To the best knowledge of the authors, this is the first time to report such model test method which can achieve similarity of both model- and full-scale thrust and torque for a wide range of wind speeds. This lays a sound foundation for achieving correct interaction during the model tests of floating offshore wind turbines in wind-wave basins. The method will be applied to such tests in our future work.

Acknowledgments

This work is sponsored by the National Natural Science Foundation of China (Nos.51739001 and 51579056), National Key Research and Development Program of China (No.2020YFB1506701), the Open Fund of the Key Laboratory of Far-shore Wind Power Technology of Zhejiang Province (ZOE20200007).

References

Azcona J., Bouchotrouch F., Gonzalez M., Garciandıa J., Munduate X., Kelberlau F., Nygaard T.A.. Aerodynamic Thrust Modelling in Wave Tank Tests of Offshore Floating Wind Turbines Using a Ducted Fan. Journal of Physics: Conference Series 524. 2014;012089(2014):1-11.

Bak C., Zahle F., Bitsche R R., Kim T., Yde A., Henriksen L.C., Natarajan A., Hansen M.. Description of the DTU 10 MW Reference Wind Turbine. DTU Wind Energy, Denmark, 2013.

Bayati I., Belloli M., Bernini L., Giberti H., Zasso A., Scale model technology for floating offshore wind turbines. IET Renewable Power Generation. 2017;11(9):1120-1126.

Bayati I., Belloli M., Bernini L., Mikkelsen R.F., Zasso A., On the aero-elastic design of the DTU 10MW wind turbine blade for the LIFES50+ wind tunnel scale model. Journal of Physics: Conference Series 753. 2016;022028(2016):1-13.

Bayati I., Belloli M., Bernini L., Zasso A., Aerodynamic design methodology for wind tunnel tests of wind turbine rotors. J. Wind Eng. Ind. Aerodyn. 2017;167(2017):217-227.

Chabaud V., Steen S., Skjetne R.. Real-time hybrid testing for marine structures: challenges and strategies. Proceedings of the ASME 2013 32nd International Conference on Ocean, Offshore and Arctic Engineering. Nantes, France, June 9-14, 2013.

Chakrabarti S.. Physical model testing of floating offshore structures. Dynamic Positioning Conference, 1998, 1-33.

Chen P., Chen J.H., Hu Z.Q., Review of Experimental-Numerical Methodologies and Challenges for Floating Offshore Wind Turbines. Journal of Marine Science and Application. 2020;19(2020):339-361.

Day A., Babarit A., Fontaine A., He Y., Kraskowski M., Murai M., Penesis I., Salvatore F., Shin H.. Hydrodynamic modelling of marine renewable energy devices: A state of the art review. Ocean Engineering. 2015;108(2015):46-69.

Duan F., Investigation on mechanism and characteristics of dynamic responses of a spar-type floating wind turbine based on model testing and numerical simulation methods. PhD thesis, Shanghai Jiao Tong University, 2017.

Du W.K., Zhao Y.S., He Y.P., Liu Y.D.. Design, analysis and test of a model turbine blade for a wave basin test of floating wind turbines. Renewable Energy. 2016;97(2016):414-421.

Faltinsen O.. Sea loads on ships and offshore structures. Cambridge university press, Cambridge, 1993.

Fowler M.J., Kimball R.W., Thomas D.A., Goupee A.J.. Design and testing of scale model wind turbines for use in wind wave basin model tests of floating offshore wind turbines. Proceedings of the ASME 2013 32nd International Conference on Ocean, Offshore and Arctic Engineering, Nantes, France, June 9-14, 2013.

Gao Z., Moan T., Wan L., Michailides C., Comparative numerical and experimental study of

two combined wind and wave energy concepts. Journal of Ocean Engineering and Science. 2016;1(2016):36-51.

Hall M., Goupee A., Jonkman J., Development of performance specifications for hybrid modeling of floating wind turbines in wave basin tests. J. Ocean Eng. Mar. Energy. 2018;4(2018):1-23.

Heronemus WE. Pollution-free energy from offshore wind. Proceedings of the 8th Annual Conference and Exposition, Marine Technology Society, Washington, DC, 1972.

Koo B.J., Goupee A.J., Kimball R.W., Lambrakos K.F., Model Tests for a Floating Wind Turbine on Three Different Floaters. Journal of Offshore Mechanics and Arctic Engineering. 2014;136(020917):1-11.

Madsen F.J., Nielsen T.R.L., Kim T., Bredmose H., Pegalajar-Jurado A., Mikkelsen R.F., Lomholt A.K., Borg M., Mirzaei M., Shin P., Experimental analysis of the scaled DTU10MW TLP floating wind turbine with different control strategies. Renewable Energy. 2020;155(2020):330-346.

Martin H.. Development of a scale model wind turbine for testing of offshore floating wind turbine systems. MSc thesis, University of Maine, 2011.

Martin H.R., Kimball R.W., Viselli A.M., Goupee A.J., Methodology for wind/wave basin testing of floating offshore wind turbines. Journal of Offshore Mechanics and Arctic Engineering. 2014;136(020905):1-9.

Sandner F., Amann F., Azcona J., Munduate X., Bottasso C.L., Campagnolo F., Robertson A., Model building and scaled testing of 5MW and 10MW semi-submersible floating wind turbines. Proceedings of the 12th Deep Sea Offshore Wind R&D Conference, EERA DeepWind'2015. Trondheim, NORWAY, February 4-6, 2015.

Sarpkaya T., Isaacson M., Mechanics of wave forces on offshore structures. J Appl Mech. 1981;49(2):466-467.

Sauder T., Chabaud V., Thys M., Bachynski E.E., Saether L.O., Real-time hybrid model testing of a braceless semi-submersible wind turbine. part I: the hybrid approach. Proceedings of the ASME 2016 35th International Conference on Ocean, Offshore and Arctic Engineering. Busan, South Korea, June 19-24, 2016.

Schunemann P., Zwisele T., Adam F., Ritschel U., Development of a scaled rotor blade for tank tests of floating wind turbine systems. Proceedings of the ASME 2018 37th International Conference on Ocean, Offshore and Arctic Engineering. Madrid, Spain, June 17-22, 2018.

Shin H.. Model test of the OC3-Hywind floating offshore wind turbine. Proceedings of the 21th International Offshore and Polar Engineering Conference. Maui, Hawaii, USA, June 19-24, 2011.

Siemens. User manual: Star-CCM+ V12.02.010. 2017

Stewart G., Muskulus M., A review and comparison of floating offshore wind turbine model experiments. Energy Procedia. 2016;94(2016):227-231.

Utsunomiya T., Sato T., Matsukuma H., Yago K., Experimental validation for motion of a SPAR-type floating offshore wind turbine using 1/22.5 scale model. Proceedings of the ASME 2009 28th International Conference on Ocean, Offshore and Arctic Engineering, Honolulu, Hawaii, USA, May 31-June 5, 2009.

Wan L., Gao Z., Moan T., Experimental and numerical study of hydrodynamic responses of a combined wind and wave energy converter concept in survival modes. Coastal Engineering. 2015;104(2015):151-169.

Wan L., Gao Z., Moan T., Lugni C., Comparative experimental study of the survivability of a combined wind and wave energy converter in two testing facilities. Ocean Engineering. 2016;111(2016):82-94.

Wan L., Gao Z., Moan T., Lugni C., Experimental and numerical comparisons of hydrodynamic responses for a combined wind and wave energy converter concept under operational conditions. Renewable Energy. 2016;93(2016):87-100.

Wan L., Greco M., Lugni C., Gao Z., Moan T., A combined wind and wave energy-converter concept in survival mode: Numerical and experimental study in regular waves with a focus on water entry and exit. Applied Ocean Research. 2017;63(2017):200-216.

Wen B.R., Jiang Z.H., Li Z.W., Peng Z.K., Dong X.J., Tian X.L., On the aerodynamic loading effect of a model Spar-type floating wind turbine: An experimental study. Renewable Energy. 2022;184(2022):306-319.

Wen B.R., Tian X.L., DongX.J., Li Z.W., Peng Z.K., Zhang W.M., Wei K.X., Design approaches of performance-scaled rotor for wave basin model tests of floating wind turbines. Renewable Energy. 2020;148(2020):573-584.

Zhao J. Numerical Simulation and Experimental Study on Hydrodynamic Characteristic of Offshore Wind Turbine System. PhD thesis, Harbin Engineering University, 2012.